Journal of Network Intelligence
Taiwan Ubiquitous Information
 ISSN 2414-8105 (Online)
Volume **6**, Number **3**, August **2021**

Intelligent Diagnosis Technology of Wind Turbine Drive System Based on Neural Network

Wei Yang*

The College of Automation, Chongqing University
Chongqing 400044, China
China Shipbuilding Industry Corporation Haizhuang Wind power Equipment CO., Ltd.
Chongqing 401122, China
Correspond Author: ywhzwindpower@126.com

Yi Chai

The College of Automation, Chongqing University
Chongqing 400044, China
State Key Laboratory of Power Transmission Equipment & System Security and New Technology, Chongqing University
Chongqing 400044, China

Jie Zheng

China Shipbuilding Industry Corporation Haizhuang Wind power Equipment CO., Ltd.
Chongqing 400044, China

Jie Liu

China Shipbuilding Industry Corporation Haizhuang Wind power Equipment CO., Ltd.
Chongqing 400044, China

Received January 2021; revised March 2021

Abstract. *Since the air pollution is becoming more and more serious, as a new type of pollution-free energy, wind energy has become more and more important. Today, almost of all countries in the world believe that wind energy is one of the future energy development trends. As the key equipment of wind power conversion, the state of wind turbine is directly related to the efficiency of wind power conversion. Therefore, the effective fault diagnosis of wind turbine drive system is the reliable guarantee of wind power generation. Based on the vibration characteristics of the wind turbine drive system, a new fault diagnosis method is established. Moreover, the fault feature extraction and classification are realized by wavelet packet decomposition and BP neural network respectively. The experimental results show that the diagnosis rate of this method is over 90%, which proves the effectiveness of this method.*
Keywords: Troubleshooting, Wind turbine, Vibration characteristic, Back propagation neural network

1. **Introduction.** As a pollution-free renewable energy source, wind energy has become one of the areas that countries around the world are competing for development. However, wind turbines are often installed in remote areas, such as mountains, wilderness, beaches and islands, and from tens of meters or even hundreds of meters from the ground. They usually work in harsh environment, such as wind speed instability, variable load, large temperature difference and low pressure for a long time. Thus, the service life of the unit is greatly shortened and affected. Especially the transmission components, such as the main shaft and gear box, are prone to failure under the action of alternating load [1-3], leading to

long-term shutdown and overhaul. Furthermore, complex operating conditions and high maintenance costs seriously damage of the economic benefits of wind power generation. On this basis, the state monitoring and fault diagnosis of wind turbines has gradually attracted the attention of the industry. Through monitoring manually, it is sometimes difficult to catch the signals of the turbine transmission system failure. It will cause maintenance personnel to misjudge the failure cause, resulting in excessive-maintenance of the undamaged parts or insufficient maintenance of faulty parts. Therefore, it is of great significance to carry out monitoring and diagnosis research on wind turbine drive system to prevent wind turbine faults and improve economic benefits.

The representative classification is divided into three categories: mathematical model based methods [4-7], data analyses based methods [8-10] and knowledge-based methods [11-14]. The benchmark model of three blade horizontal axis wind turbine was established [4]. Five different fault monitoring and isolation schemes were used to evaluate seven different test series and obtain satisfactory results. However, the simplification of the benchmark model cannot reflect the complex functions of wind turbine. In the research of fault diagnosis methods for wind turbines based on signal processing, [15] proposed a wind turbine fault diagnosis method. Use Continuous Wavelet Transform (CWT) to filter out unnecessary noise in the original vibration signal, and use Automatic Term Window (ATW) functions to suppress cross terms in Wigner-Ville Distribution (WVD), which may be caused by moisture absorption, fatigue, gusts or lightning strikes on the wind turbine. Meanwhile, damaged faults are also analyzed and diagnosed. Liu et al. [16] proposed a new wind turbine fault diagnosis method based on Local Mean Decomposition (LMD) technology. LMD is a new method of iterative demodulation of amplitude and frequency modulation signals, which is suitable for obtaining instantaneous frequencies in the condition monitoring and fault diagnosis of low-speed wind turbines. Through the experimental analysis of the vibration signal of the wind turbine, the validity and effectiveness of the method are verified. After decades of development, neural network theory has achieved extensive success in many research fields, such as pattern recognition, automatic control, signal processing, assistant decision-making [13] and artificial intelligence. The following introduces the application status of neural network in fault diagnosis. The neural network was applied to wind turbine fault detection and identification [11,12], and the results show that this method has the advantages of high efficiency, strong robustness and strong anti-noise interference ability. In order to suppress the local minimum problem, Wang [17] combined Wavelet Packet Analysis with Radial Basis Function neural network and applied it to the fault diagnosis of wind turbine transmission system. In terms of convergence, approximation ability and classification ability, this method has no comparable advantages.

This paper analyzes the wavelet packet decomposition of the vibration signal of the wind turbine drive system and its frequency characteristics. It is found that the frequency energy distribution of different parts is the same, the middle and low frequency energy is the majority and the extracted features are back propagation (BP) nerve. The network classification results show that the detection accuracy of rolling element fault, inner ring fault and outer ring fault is 97%, 92% and 99% respectively.

2. **Method.**

2.1. **System Framework.**

First, vibration signals of collected key components are preprocessed, and the singular value decomposition and noise reduction method are applied to improve the signal-to-noise ratio of the vibration signal. Then, time-frequency analysis of the denoised signal is performed based on the wavelet packet energy entropy to extract

the characteristic parameters and the extracted parameters. The characteristic parameter is set as the input of BP network to realize the automatic diagnosis of the failure. The detailed method is shown in Fig. 1:

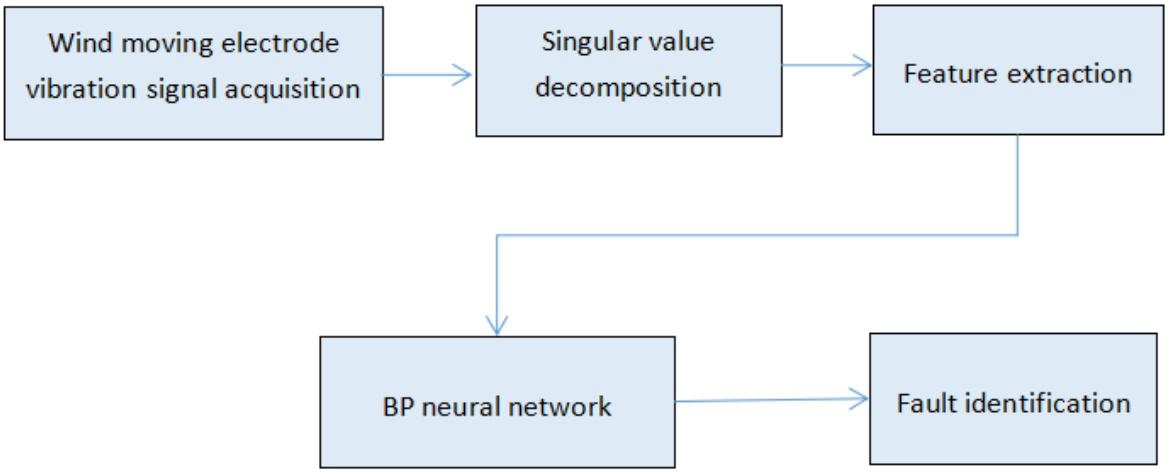

FIGURE 1. The framework of analysis process

The vibration signal acquisition system hardware includes sensors, data acquisition instruments, notebook computers and connecting cables. The vibration data acquisition instrument adopts BENTLY 8-channel vibration signal acquisition instrument, vibration signal acquisition system.

2.2. **Singular Value Decomposition.** Due to the large number of vibration sources and noise interference, the key information contained in the collected signal is easily concealed. Therefore, the signal should be denoised before taking the signal characteristics. Signal noise reduction is a key step in signal processing and troubleshooting. In engineering practice, there are many different noise reduction techniques that can be applied. Wavelet noise reduction, time domain averaging, frequency domain feature extraction and adaptive filtering are commonly used. However, these methods have their own limitations. When the wind turbine drive system fails, shock signals appear in the vibration signal. These shock signals are coupled with noise and other vibration signals. Thus, it is difficult to extract the noise by general noise reduction method. Aiming at this problem, this paper proposes a vibration signal denoising method by singular value decomposition to filter the collected noisy signals. Assuming the collected noisy vibration signal is, the phase space reconstruction theory is used to embed the elements of $X = [x(1), x(2), \ldots, x(n)]$ into the m*n dimensional space to obtain a Hankel matrix. According to singular value decomposition principle, given any m*n-dimensional matrix A, singular value decomposition can be expressed as Eq.1:

$$A = U\Sigma V^t = U \begin{bmatrix} \sum r & 0 \\ 0 & 0 \end{bmatrix} V^T \tag{1}$$

In Eq.1, U and V are orthogonal matrices of m*n and n*m respectively,
$\sum r = \text{diag}\,(\lambda_1, \lambda_2, \ldots, \lambda_r)$ and $\lambda_1 > \lambda_2 > \ldots > \lambda_r$, $r = \text{rank}(A)$.

The energy information of the signal and the noise intensity information are all included in singular spectrum. Furthermore, the use of singular spectrum can realize the separation of useful signals and interference signals. The set signal X is composed of two parts: noise-free and noise. The noise-free signal should be smooth, and the noise signal is Gaussian.

Therefore, the singular value of signal X is also composed of two parts: noise-free singular values and singular values of noise. Then the singular value of the entire noise will be evenly offset from the original size .

At this point, the trajectory matrix of signal X can be expressed as Eq.2:

$$A = [U_1 U_2] \begin{bmatrix} 1 & 0 \\ 0 & \sum r \end{bmatrix} \begin{bmatrix} V_1^T \\ V_2^T \end{bmatrix} \tag{2}$$

In Eq.2, it can be seen that by decomposing singular value of trajectory matrix, A can be divided into two parts. As long as the noise interference part is removed, the effective signal part can be obtained. The basic steps of noise reduction for singular value decomposition are as follows:

Firstly, phase space reconstruction is performed on the original signal. The reconstructed matrix line number is half or one tenth of the original signal length. Then, the Hankel matrix obtained is subjected to singular value decomposition, and the singularity corresponding to each step of the singular spectrum is obtained. The entropy increment determines the order in which the singular entropy increment begins to decrease and tends to be stable as the signal denoising order. The matrix is reconstructed by using the previously obtained noise reduction order as the effective order of the singular spectrum. The first row element of the reconstructed matrix is the noise reduction signal.

2.3. **Wavelet Packet Energy Entropy Characteristics.** As a signal processing method, wavelet packet analysis is extended of wavelet analysis, which can reconstruct and process the signal in more detail. The advantage of wavelet packet analysis is that the approximate signal is further decomposed and reconstructed in the wavelet transform, and then the high-frequency part of the signal is analyzed. Because the orthogonal wavelet transform can only further analyze the low-frequency part of the signal and cannot continue to decompose the high-frequency part, the wavelet transform can represent the low-frequency information well, but the effect is not very good. Ground decomposition and representation of high frequency signals contain a large amount of detail information.

The vibration signal of wind turbine drive system is a typical non-stationary signal with a lot of detailed information. It can be processed in a more detailed way by using wavelet packet transform. This decomposition has no redundancy or even omissions, which is a better time-frequency localization analysis method. More specifically, wavelet packet analysis can not only obtain the distribution information of the original signal in different frequency bands, but also capture the time point of the signal mutation by decomposing and reconstructing the signal at different scales.

The wavelet packet decomposition is essentially the multi-layer bisection of the high-frequency sub-segment and the low-frequency sub-segment divided by the original signal. In this paper, noise-reduced signal is decomposed by wavelet packet. In view of the decomposition relationship, the wavelet packet divides the signal into eight frequency bands, and the decomposition of high-frequency part is more detailed. Thus the noise-reduced signal can be fully utilized. Wavelet packet analysis decomposes non-stationary signal into a series of basic functions that are stretched by wavelet function. The information is complete, which is very suitable for the decomposition of vibration signals.

After 3-layer decomposition of the signal, the wavelet energy of the sub-channel signal can be expressed as Eq.3:

$$E_{3j} = \int |S_{3j}(t)|^2 \, dt = \sum_{k=1}^{n} |x_{jk}|^2 \tag{3}$$

In Eq.3, represents the discrete point amplitude of the reconstructed signal .

The magnitude of the energy entropy represents how much energy is ordered in the observed signal. When the number of wavelet packet decomposition layers is defined as, the energy sum of the signals is , and it can be expressed as Eq.4:

$$E_i = \sum_{j=0}^{N} E_{ij} \tag{4}$$

Depending on the law of energy conservation, the total energy of signal is equal to the sum of signal energies of sub-bands, which can be expressed as Eq.5:

$$E_s = E_i = \sum_{j=1}^{N} E_{ij} \tag{5}$$

The great uncertainty of the variable means high entropy, and the great amount of information needs to be explained. For spectrum analysis, different frequency bands reflect different characteristic information. Therefore, specific information entropy based on the characteristics of frequency distribution is applied to reflect fault. The entropy is identified as Eq.6:

$$H(x) = E\left[\log_2 \frac{1}{P(x_i)}\right] = -\sum P(x_i) \log_2 P(x_i) \tag{6}$$

Where, is output probability function and represents the random variable. It is defined as a symbol set and is the set of all possible outputs.

In frequency domain, vibration signals of segments present the component of mechanical structure. Frequency segments of wind turbine can be divided into low-frequency 10-1000Hz, mid-frequency 1000-2000Hz and high-frequency 2000-10000 respectively. In this paper, frequency domain is subdivided into eight segments. After decomposition, the mutation phenomenon is reduced.

2.4. **BP Neural Network.** BP algorithm has the characteristics of simple structure and easy implementation. More importantly, its excellent pattern recognition ability has also been widely used in mechanical diagnosis. The learning process of BP neural network consists of two parts: the forward propagation of signal and the back of error.

From the input layer, the error is generated by the result of the forward propagation and the expected value, which is allocated to the nodes of each layer through back propagation for weight modification until the error is lower than a recognized level or a predetermined learning time. Distinctive faults produce specific vibration signals. The neural network-based fault classification extracts the characteristics of the fault signal by training weights.

3. Data Sources.

3.1. **Vibration Signal.** The vibration signal acquisition system hardware includes sensors, data acquisition instruments, notebook computers and connecting cables. The vibration data acquisition instrument adopts NEGO 8-channel vibration signal acquisition instrument, and the vibration signal acquisition system is shown in Fig. 2.

The signal is the carrier of fault information, and the measuring point is the window to obtain the fault information. The pros and cons of the arrangement of measuring points will determine whether the collected signal is typical and representative. The rationality of the measuring point selection is the basis for subsequent signal analysis and processing. When collecting wind turbine signals, the selection of measuring points must be in accordance with the international standard VDI3834, and the following principles shall be met:

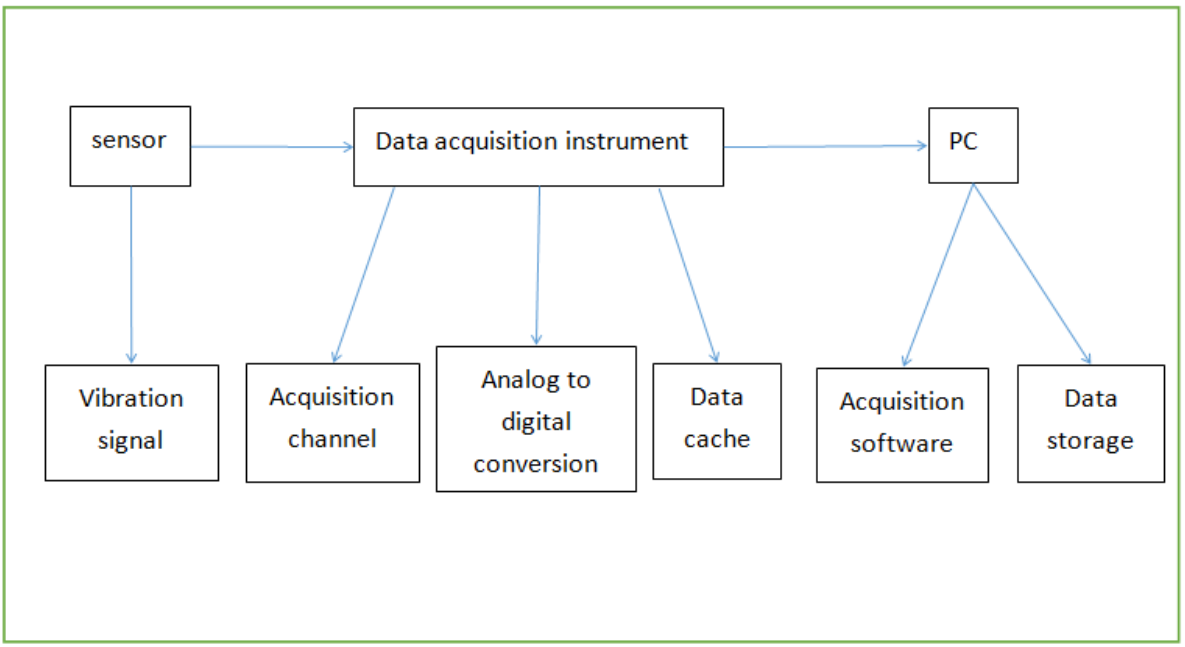

FIGURE 2. The framework of analysis process

1) The measuring point should try to select the most abundant part of the vibration information;

2) Select as many working conditions as possible with few points and maintain sensitivity to the measured parameters;

3) The position of the measuring point should be close to the tested part to prevent attenuation, distortion and transmission obstruction;

4) The selection of measuring point position should consider the convenience of assembly and disassembly of the sensor. The choice of measuring point position should consider the convenience of disassembly and assembly of the sensor.

Take Hansen EH80421-BN gearbox of 2MW wind turbine, the main structure includes the main shaft, planetary-stage gear and two parallel gears. The geometric shapes of the parallel gears used in the planetary gear system and gearbox are shown in Table 1.

TABLE 1. Geometrics of the planet gears (High Shaft Speed is 26.67Hz)

Parametre	Sun Gear	Planet Gear	Ring Gear	Carrier	LS Big Gear	IM Small Gear	IM Big Gear	HS Small Gear
Number of teeth	18	34	87	-	70	16	84	19
RPM	82.72	50.47	-	14.18	82.72	361.91	361.91	1600
Hz	1.38	0.84	-	0.24	1.38	6.03	6.03	26.67
Meshing frequency	20.562	20.562	20.562	20.562	96.508	96.508	506.668	506.668

The vibration sensor is 8071LF-01-010 MEAS, whose parameter description is introduced in Tab. 2. The data acquisition process is as follows: acceleration of vibration signal collected by sensors is converted into electrical signal. Then the data are transmitted to server by digital signals. Fig. 3 shows the positions of nine vibration sensors and diagram of gearbox structure. Actual field installation is displayed in Fig. 4.

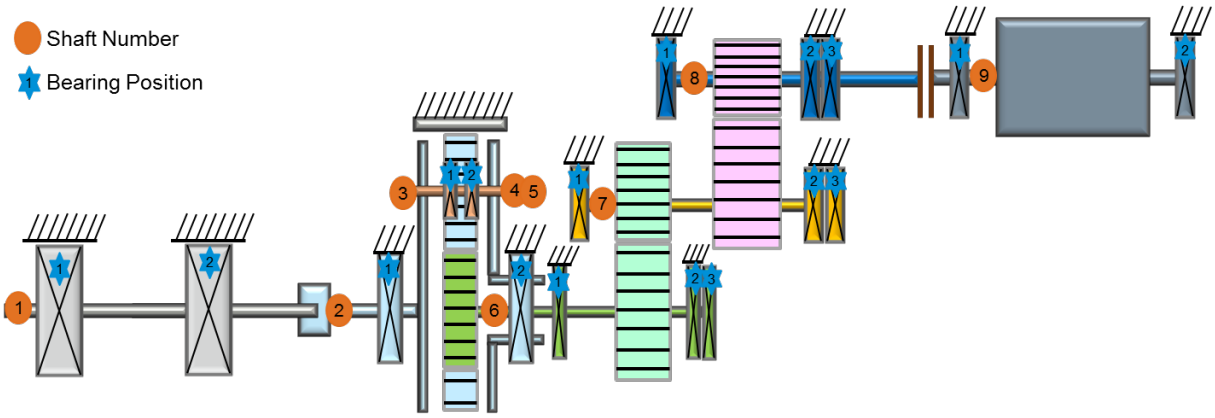

FIGURE 3. The framework of analysis process

Finally, a small amount of vibration data is shown as Tab. 3, which is collected from the horizontal direction of high-speed shaft of the Hansen.

FIGURE 4. The framework of analysis process

3.2. **Noise Reduction.** In order to improve the signal-to-noise ratio, denoising is necessary. In this paper, singular value decomposition (SVD) is used to decompose the signal into effective signal with large singular value and noise with small singular value. The noise is eliminated by setting zero to the latter. When the noise is tiny, the singular value displays obvious step distribution. Singular value decomposition order and the separation order are significant to the denoising results. Figure 5 shows the original state and denoising effect of gearbox vibration signal.

3.3. **BP Neural Network Layers of Neurons.** For both the rotor and bearing fault identification, 8 Shannon entropy and 6 time domain indicators are selected as input vectors, so the input node of BP neural network should be 14. For the output layer, three working conditions of the rotor and the four working conditions of the bearing are identified respectively. Therefore, output nodes of the network are set to 3 and 4

TABLE 2. Vibration data

NO.1	NO.2	NO.3	NO.4	NO.5	NO.6	NO.7	NO.8	NO.9
0.0957	-0.006	-1.7048	-1.2262	4.4563	-1.0468	70.972	-14.326	-11.395
0.0239	0.0179	1.1066	-0.2094	-0.5683	1.3459	-49.8569	-10.3781	-5.2937
-0.1316	0.0179	3.4993	0.2094	-0.8075	2.3029	77.1929	-11.2156	-18.8122
-0.0718	0.0179	5.3536	0.6281	-0.9272	5.1741	-80.0043	13.4288	28.2034
-0.1794	0.0419	6.9686	-0.2094	-2.1235	6.7891	43.5762	-10.6772	-5.6526
-0.0957	0.1137	6.5499	-0.2094	-2.4226	-1.8842	-46.9259	-2.3029	33.5868
-0.1316	0.1974	3.7983	-1.3459	-0.6281	4.3965	36.8169	-14.326	40.047
-0.1196	0.2811	0.8075	-2.5422	-3.0207	-0.6281	-55.6591	-16.3598	10.7968
-0.1555	0.317	-1.1066	-2.9011	0.7477	-3.0805	-23.2386	-0.4486	24.1359
-0.1436	0.3051	-2.4226	-2.602	1.2262	-6.3106	-39.0899	7.3873	-3.4394

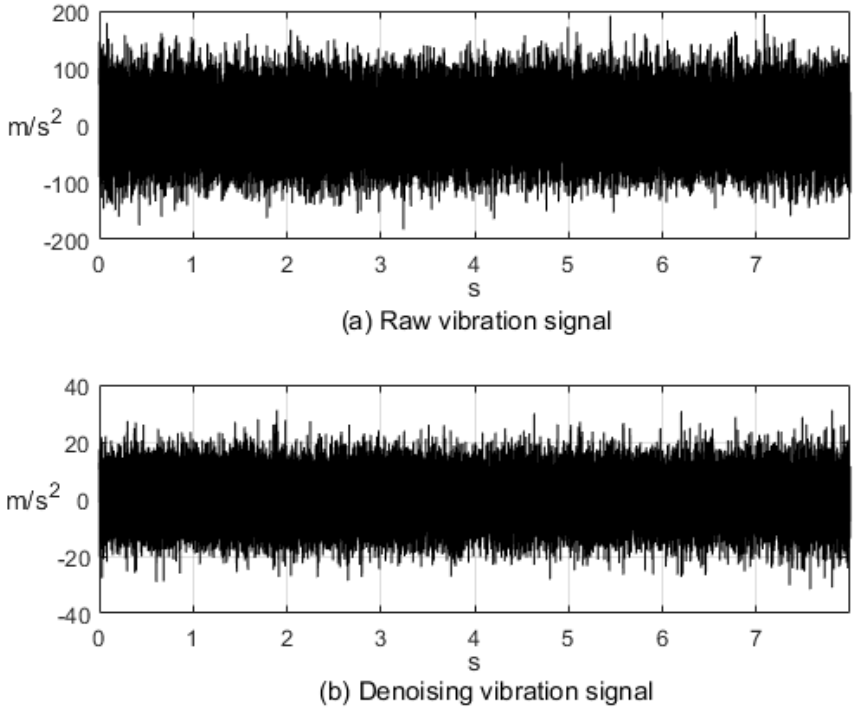

FIGURE 5. The framework of analysis process

respectively. The determination of hidden layer neurons is determined according to Eq.7, Eq.8 and Eq.9:

$$m < \sqrt{n+l} + \alpha \tag{7}$$

$$m = \log_2 n \tag{8}$$

$$m = \log_2 nm < n - 1 \tag{9}$$

In Eq.7, Eq.8 and Eq.9, m and n represent the node number of hidden layer and input layer respectively, and l is used to represent the number of output layer nodes. Normally, is a constant between 1 and 10. The eigenvector training samples are input into BP neural network for training. Furthermore, the global error is 0.01 and the maximum number of training set is 1000.

Shannon entropy represents the information of eight frequency segments. In other words, the low-frequency entropy represents the state of the main shaft and planetary gears. Similarly, the characteristics of parallel gears are also reflected in the middle section.

There are six indicators in time domain. First, effective value represents the whole vibration energy. In addition, the margin indicator increases obviously with the increase of vibration. In order to describe the impact, kurtosis and pulse index are calculated. On the other hand, peak value indicates surface roughness of the bearing. In particular, the waveform indicator is the root mean square value divided by the absolute average.

4. **Results.**

4.1. **Gearbox Bearing Vibration Signal.**

The gearbox bearing data set contains all aspects of bearing mechanical state information, including different bearing fault locations, fault levels, fault bearing positions and different workload. Therefore, the data set can be used from multiple perspectives and different classifications. Experiments are tested to verify effectiveness of the proposed method.

The three-layer decomposition of the wavelet divides the frequency of signal into 8 parts according to the average from low to high. Fig. 6 shows the energy distribution of 8 signals after different wavelet decomposition. After the wavelet packet decomposition, the normal non-fault is presented in the figure. If the fault occurs, the frequency distribution is not uniform. In these three kinds of wind turbine drive system, rolling element fault, inner and outer ring fault are common fault types. The fault energy distribution has great similarity and is basically concentrated in the low frequency range. The distribution evaluation rate of low frequency 2, 3 and 4 frequency segments is the highest, and the rolling fault is the lowest compared with the other two faults. The frequency segment energy distribution is lower than the other two faults.

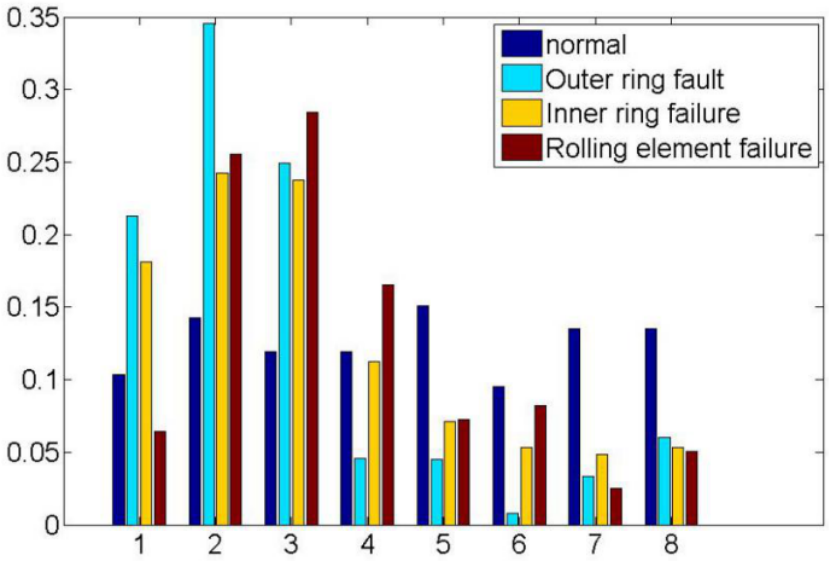

FIGURE 6. The framework of analysis process

In a healthy state, vibration frequency domain of the bearing reflects the mechanical structure in wind turbine gearbox. For smooth running turbine, the information in each segment is homogeneous. Otherwise, the entropy of high frequency comes from the higher harmonic of vibration.

Bearing failure accompanied by 1X or other bearing failure frequency sidebands. The failure of the inner and outer ring precedes the rolling body and the cage. The retainer fracture causes in the appearance of Rolling Element Defect Frequency (BSF) and Cage Defect Frequency (FTF) of retainer fault frequency. When the rolling body fails, several times of BSF will be generated. Furthermore, the inner and outer ring faults produce their own fault characteristic frequencies.

In normal condition, the expectation is 4.514 and the variance is 0.0002705. Obviously, Shannon entropy distribution of the bearing vibration signal is relatively uniform. Tab. 3 illustrates the variances and expectations of four entropy distributions.

TABLE 3. Vibration signal entropy analysis

Case	Expectation	Variance
Normal	4.514	0.0002705
Outer ring fault	2.819	0.0138
Inner ring fault	3.192	0.0069
Rolling element failure	3.510	0.0088

When fault occurs, a lot of fault characteristic information appears in the low frequency band, which results in the decrease of higher-frequency proportion. It can be noticed that the variance of the outer ring reaches 0.0138, and the proportion is highly attenuated in region 6. Correspondingly, the Shannon entropy of the inner ring fault is dominant in band 2 and band 3. However, the expectation caused by rolling body fault is 3.510.

4.2. **Fault Identification Results.** In order to verify the proposed method, fifty Hanse gearboxes of wind turbines with different degrees of bearing wear are tested. The tests are operated with MATLAB code on a PC with fourth-generation i7 CPU and 16GB of RAM.

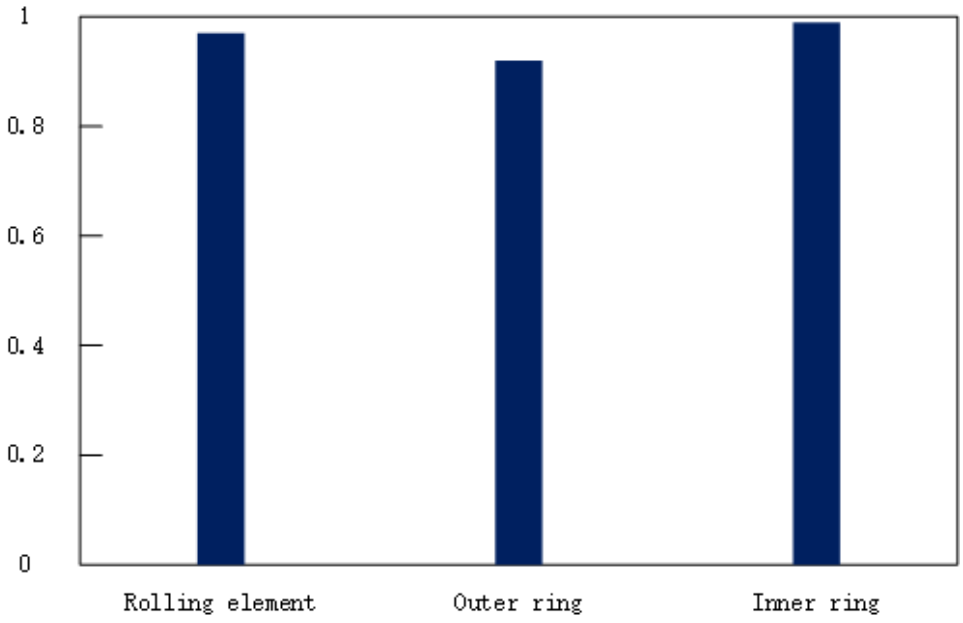

FIGURE 7. The framework of analysis process

The generators driven by wind turbines run at about 1600 rpm with 2 MW. To obtain detailed condition of bearing wear, signals are sampled constantly. The accelerometer is

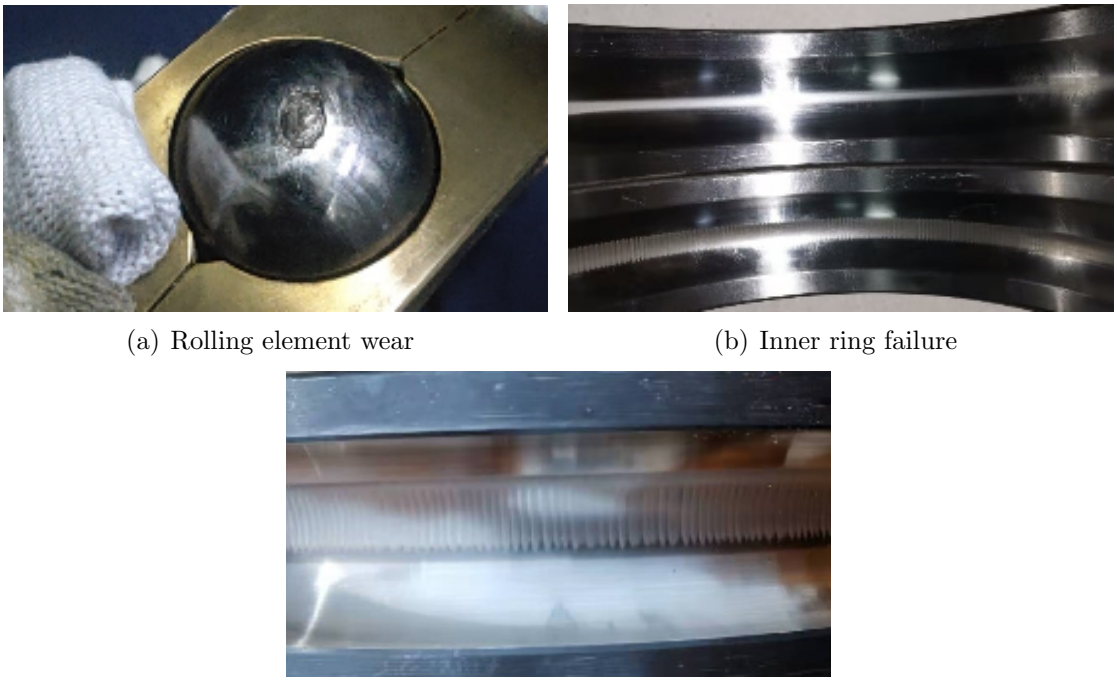

(a) Rolling element wear

(b) Inner ring failure

(c) Outer ring failure

FIGURE 8. Main name

stuck on the bearing seat, and the vibration signal is collected at a sampling frequency of 16384hz. The collected gearbox vibration signals are stored on server by the on-line condition monitoring systems. Particularly, the output shaft frequency is 26.67 Hz.

Fig. 7 shows the accuracies of fault detection for three parts, which are 97%, 92% and 99% respectively. In order to verify the correctness of the fault detection, the gearbox bearing is disassembled as shown in Fig. 8. The results show that the method can well identify the bearing faults of wind turbine.

5. **Conclusions.** The vibration signal generated by the wind turbine drive system during operation contains important equipment status information. This paper selects vibration signal of wind turbine drive system as the research object, and extracts the fault characteristics to realize fault diagnosis of the wind turbine drive system. Based on the characteristics of vibration signal, this paper uses wavelet packet decomposition method to solve the frequency distribution of different faults, and then carries out feature extraction. Then the fault types are realized by BP neural network. The experimental results prove that the method is more accurate than single-variable diagnosis. It provides a new idea and method for the fault diagnosis of the unit drive system.

REFERENCES

[1] H. Chen, S. Jing, X. Wang, Z. Wang, Fault Diagnosis of Wind Turbine Gearbox Based on Wavelet Neural Network, *Journal of Low Frequency Noise Vibration and Active Control*, vol.37, no.4, pp.977–986, 2018.

[2] J. Cheng. C. He, Y. Lyu, Y. Zheng, L. Xie, Method for Evaluation of Surface Crack Size of Wind Turbine Main Shaft by Using Ultrasonic Diffracted Waves, *Smart Materials and Structures*, vol.29, no.7, 075009, 2020.

[3] J. H. Kang, H. W. Lee, Study on the design parameters of a low speed coupling of a wind turbine, *International Journal of Precision Engineering and Manufacturing*, vol.18, no.5, pp.721-727, 2017.

[4] P. F. Odgaard, J. Stoustrup, M. Kinnaert, Fault tolerant control of wind turbines - A benchmark model, *IFAC Proceedings Volumes (IFAC-PapersOnline)*, vol.42, no.8, pp.155–160, 2009.

[5] C. Liu, X. Meng, H. Zhang, Research of binocular positioning mathematical model based on the least square method, *Applied Mechanics and Materials*, vol.50, pp.473–477, 2011.
[6] Q. Jiang, Q. Sui, J. Wang, Technical and experimental study of fiber Bragg grating vibration detection based on matching demodulation method, *In Proceedings of the IEEE International Conference on Automation and Logistics*, pp.1299–1303, 2007.
[7] M. Ruiz, L. E. Mujica, S. Alférez, L. Acho, C. Tutivén, Y. Vidal, J. Rodellar, F. Pozo, Wind turbine fault detection and classification by means of image texture analysis, *Mechanical Systems and Signal Processing*, vol.107, pp.149–167, 2018.
[8] K. P. Kumar, K. V. N. S. Rao, K. R. Krishna, B. Theja, Neural network based vibration analysis with novelty in data detection for a large steam turbine, *Shock and Vibration*, vol.19, no.1, pp.25–35, 2012.
[9] M. Frizzarin, M. Q. Feng, P. Franchetti, S. Soyoz, C. Modena, Damage detection based on damping analysis of ambient vibration data, *Structural Control and Health Monitoring*, vol.17, no.4, pp.368–385, 2010.
[10] D. García, I. Trendafilova, A multivariate data analysis approach towards vibration analysis and vibration-based damage assessment: Application for delamination detection in a composite beam, *Journal of Sound and Vibration*, vol.333, no.25, pp.7036–7050, 2014.
[11] X. An, D. Jiang, S. Li, Application of back propagation neural network to fault diagnosis of direct-drive wind turbine, *In Proceedings of 2010 World Non-Grid-Connected Wind Power and Energy Conference*, pp.101–105, 2010.
[12] A. Adouni, D. Chariag, D. Diallo, M. B. Hamed, L. Sbita, FDI based on Artificial Neural Network for Low-Voltage-Ride-Through in DFIG-based Wind Turbine, *ISA Transactions*, vol.64, pp.353–364, 2016.
[13] E. K. Wang, S. P. Xu, C. Chen, N. Kumar, Neural-Architecture-Search Based Multiobjective Cognitive Automation System, *IEEE Systems Journal*, vol.15, no.2, pp.2918-2925, 2020.
[14] K. Z. Tang, K. K. Tan, C. W. D. Silva, T. H. Lee, K. C. Tan, S. Y. Soh, Application of vibration sensing in monitoring and control of machine health, *In IEEE/ASME International Conference on Advanced Intelligent Mechatronics*, pp.377–382, 2001.
[15] B. Tang, W. Liu, T. Song, Wind turbine fault diagnosis based on Morlet wavelet transformation and Wigner-Ville distribution, *Renewable Energy*, vol.35, no.12, pp.2862–2866, 2010.
[16] W. Y. Liu, W. H. Zhang, J. G. Han, G. F. Wang, A new wind turbine fault diagnosis method based on the local mean decomposition, *Renewable Energy*, vol.48, pp.411–415, 2012.
[17] X. Y. Wang, Fault diagnosis on transmission system of wind turbines based on wavelet packet transform and RBF neural networks, *Applied Mechanics and Materials*, vol.373-375, pp.1102–1105, 2013.